EUROFUSION WPS1-PR(16) 16771

G. A. Wurden et al.

Limiter Heat Loads during the first operation of the W7-X stellarator

Preprint of Paper to be submitted for publication in
Nuclear Fusion

This work has been carried out within the framework of the EUROfusion Consortium and has received funding from the Euratom research and training programme 2014-2018 under grant agreement No 633053. The views and opinions expressed herein do not necessarily reflect those of the European Commission.

This document is intended for publication in the open literature. It is made available on the clear understanding that it may not be further circulated and extracts or references may not be published prior to publication of the original when applicable, or without the consent of the Publications Officer, EUROfusion Programme Management Unit, Culham Science Centre, Abingdon, Oxon, OX14 3DB, UK or e-mail Publications.Officer@euro-fusion.org

Enquiries about Copyright and reproduction should be addressed to the Publications Officer, EUROfusion Programme Management Unit, Culham Science Centre, Abingdon, Oxon, OX14 3DB, UK or e-mail Publications.Officer@euro-fusion.org

The contents of this preprint and all other EUROfusion Preprints, Reports and Conference Papers are available to view online free at http://www.euro-fusionscipub.org. This site has full search facilities and e-mail alert options. In the JET specific papers the diagrams contained within the PDFs on this site are hyperlinked

Limiter Observations during W7-X First Plasmas

G. A. Wurden[a], C. Biedermann[b], F. Effenberg[c], M. Jakubowski[b], L. Stephey[c], S. Bozhenkov[b], S. Brezinsek[d], B. Cannas[e], F. Pisano[e], H. Niemann[b], S. Marsen[b], H. P. Laqua[b], R. König[b], O. Schmitz[c], J. H. Harris[f], E. A. Unterberg[f], and the W7-X Team[b]

[a]Los Alamos National Laboratory, PO Box 1663, Los Alamos, NM 87545 USA

[b]Max Planck Institut für Plasma Physik, Wendelsteinstr. 1, 17491 Greifswald, Deutschland

[c]University of Wisconsin, Madison, WI, 53706 USA

[d]Forschungszentrum Jülich GmbH, IEK-4 Jülich, Deutschland

[e]University of Cagliari, Via Universita 40, 09124 Cagliari, Italy

[f]Oak Ridge National Laboratory, PO Box 2008, Oak Ridge, TN 37831 USA

E-mail: wurden@lanl.gov

Abstract. During the first operational phase (OP1.1) of the new Wendelstein 7-X (W-7X) stellarator, five poloidal graphite limiters on the inboard side of the vacuum vessel (one in each of the W7-X modules) served as the main boundary for the plasma. Each limiter consisted of nine specially shaped graphite tiles, designed to conform to the last closed field line geometry in the bean-shaped section of the standard OP1.1 magnetic field configuration. We observed the limiters with multiple infrared and visible camera systems, as well as filtered photomultipliers. Power loads are calculated from IR temperature measurements using THEODOR, and heating patterns (dual stripes) compare well with field line mapping and EMC3-EIRENE predictions. While the poloidal symmetry of the heat loads was excellent, the toroidal heating pattern showed up to a factor of 2x variation, with peak heat loads on Limiter 1. The total power intercepted by the limiters was up to ~ 60% of the input ECRH heating power. Calorimetry using bulk tile heating (measured via post-shot IR thermography) on Limiter 3 showed a difference between short high power discharges, and longer lower power ones, with regards to the fraction of energy deposited on the limiters. Finally, fast heating transients, with frequency > 1kHz were detected, and their visibility was enhanced by the presence of surface coatings which developed on the limiters by the end of the run.

1. Introduction

During the first operational phase (OP1.1) of the new W7-X stellarator, specially shaped poloidal graphite limiters, each consisting of nine discrete tiles, served as the main plasma facing component (Figure 1), with one limiter per module [1,2]. They were located on the inboard side of the modules at the bean-shaped plasma cross-section. We used a variety of instruments to monitor the status of the five limiters, including a dedicated set of diagnostics to observe their performance and infer basic transport behaviour of the 3-D helical SOL plasma. In addition to a set of low resolution near-IR cameras [3], we had [4] an infrared (FLIR SC8303HD) camera (3-5 um band, 125 Hz full-frame rate, 1344x768 pixels) and an AVT Prosilica GX-1050C (400-800 nm, 100 Hz full-frame rate, 1024x1024 pixels) color visible camera co-located on the same line of sight in Module 3. An 8-12 um DIAS IR camera

(50 Hz, 640x480 pixels) viewed one side of Limiter 5 [5]. Near-IR cameras viewed Limiters 1 and 5 from the ECRH launcher positions [1]. A filterscope (24 channels of filtered photomultipliers watching 5 fiber optics positioned around the torus) had one fiber directly viewing part of Limiter 3 [6]. These instruments enabled us to develop information on edge plasma and wall conditions, and provided input for edge plasma codes to enable a beginning of our understanding of the plasma wall interactions in the W7-X stellarator. This paper focuses on high resolution infrared observations, which enabled heat flux and power loading estimates on the limiters.

2. Results

2.1 General features

The first helium plasmas (in Dec 2015), were small in diameter and highly radiating, and consequently the limiters initially received little deposited energy (only a few °C surface temperature increase). In fact, in the very first plasma (a helium discharge), the cold, collapsing discharge nicely illuminated the field line directions right above the tiles on limiter 3, as seen in the color image of Limiter 3 in Figure 1 (middle).

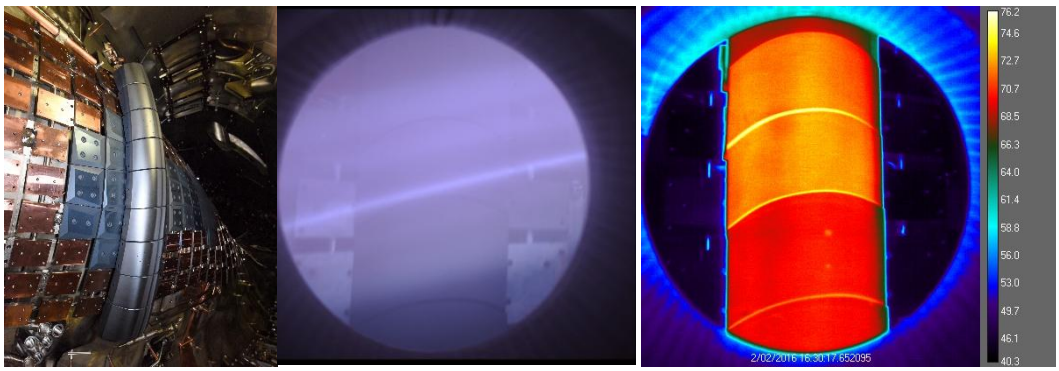

Figure 1. (left) Side view of Limiter 5. (middle) True color image of the first helium discharge in W7-X (Dec. 10, 2015), showing the local magnetic field line angle above the limiter mid-plane, Limiter 3. (right) AEA30 port, FLIR IR camera view of Limiter 3, tiles 2 thru 6, between shots (Feb 2, 2016). Two defect spots can be seen on tile 5.

Then plasmas improved as we conditioned the walls with helium glow discharge cleaning (prior to energizing the superconducting coils), and repetitive hydrogen plasmas between main pulses. Discharges grew in diameter (to fully contact the limiters), in pulse length (up to 6 seconds), in power and input energy (up to 4 MW and 4 Megajoules). Dual contact stripes on the limiter surface became the dominant infrared feature, as shown in Figure 2. The stripes have a separation of 5.5-6 cm, and a FWHM of 4-4.5 cm (which is important for later visual comparison of the erosion/deposition patterns).

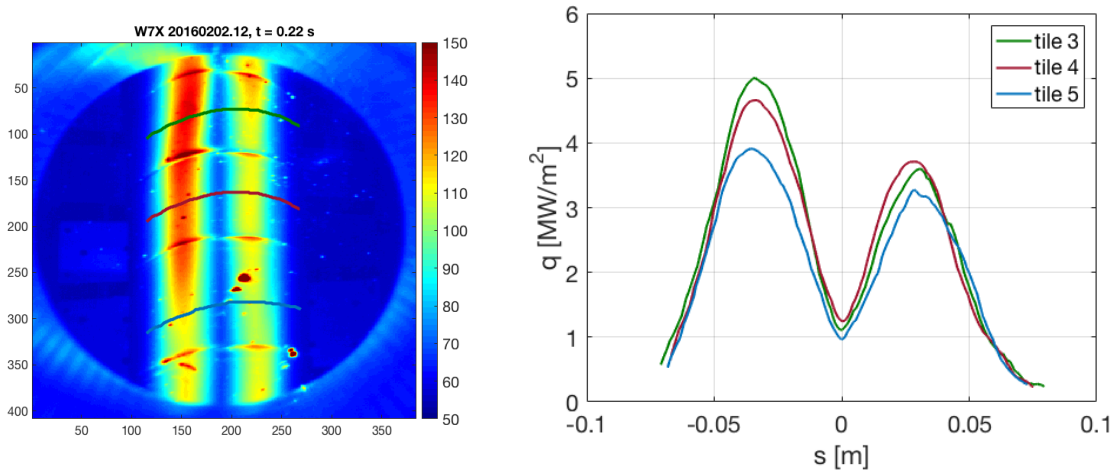

Figure 2. (left) Typical dual-stripe IR heating pattern (temperature ºC) seen on the Limiter 3 central tiles (20160202.012). (right) Calculated heat flux profiles (away from leading edge effects) along curved surface coordinates (green, red, blue lineout overlay) across tiles 3, 4, & , respectively.

During a pulse, the tile surface temperatures increased as the square root of time, during shots with constant heating power, as expected from energy impinging on uncooled "semi-infinite" solids. As predicted [1,2], the highest points or "watershed" of the curved limiters between the two heating stripes did not intercept much energy. Also, the lower leading edge on the left side of each tile, and the upper edge on the right side of each tile received the highest heat fluxes, a pattern consistent with particle transport along the magnetic field lines. Sometimes blooming behaviour could be seen, in addition to the power stripes, as shown in Figure 3.

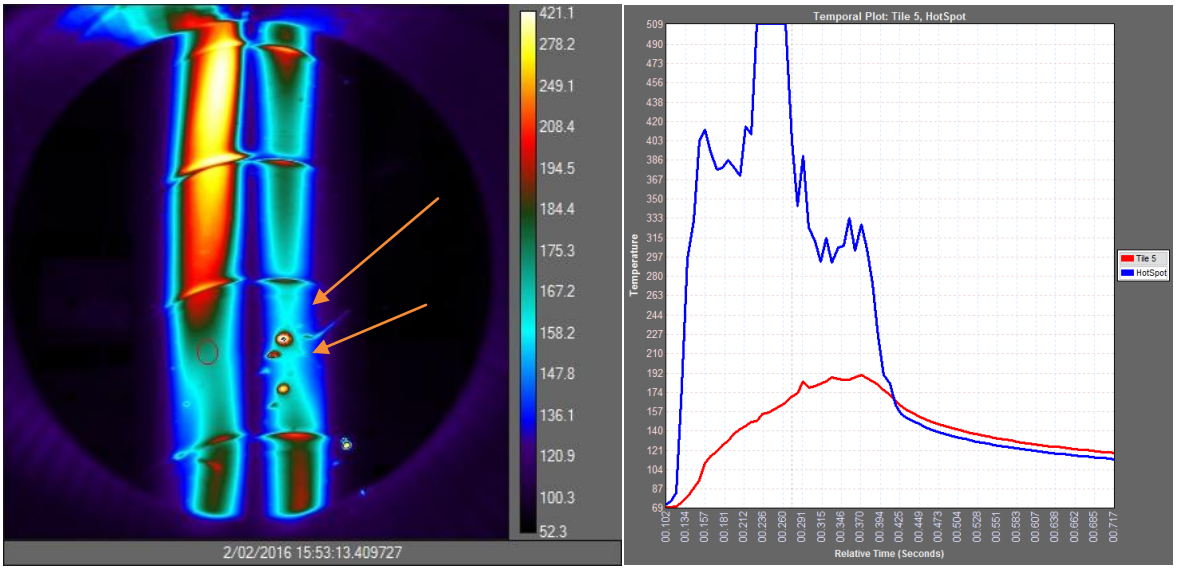

Figure 3. (left) Shot 20160202.023, Limiter 3 infrared temperature image. Two defect hot spots (arrows), > 500 °C, can be seen on the right power stripe, emitting debris. Poor thermal contact compared to bulk tile regions (red trace) is evidenced by their rapid rise /fall time history (blue trace).

On Limiter 3, tile 5 (the middle tile, with our numbering convention taken as 1 through 9, top to bottom), there were two hot spots (>500 °C) (Figure 3.), which occasionally showed real carbon bloom behaviour, consisting of hot material (tiny IR UFO's) flying from them, and bright emission in CIII light, as observed with the Prosilica visible camera (see Figure 4a). These imperfections were present in pre-run visible light images, and behaved as if they had reduced thermal contact to the bulk material.

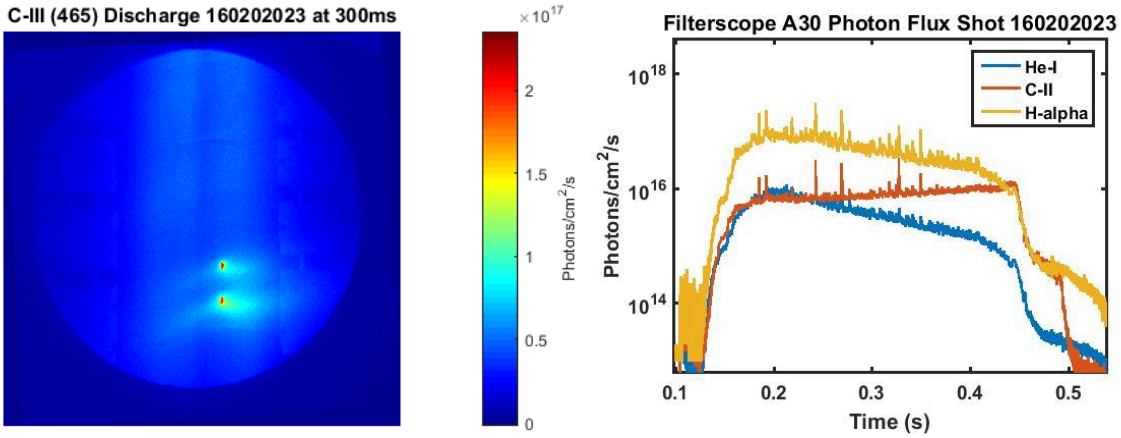

Figure 4. Shot 201600202.023 A 4 MW short pulse hydrogen plasma. (a).(left) Two carbon blooms in CIII light from tile 5, limiter 3. (b). (right) Filtered photomultiplier time traces looking directly at the Module 3 limiter (AEA30 port), showing some fluctuations (but not looking at the blooming spots).

A 24-channel filterscope, consisting of filtered photomultipliers fed by fiber-optics, has been used for first measurements at W7-X [6]. Spatial channels at five different port locations have been split into four spectral channels each-- C-II (515 nm), H-beta (486 nm), He-I (667 nm), and H-alpha (656 nm). Each viewing chord has a width of approximately 2.5 cm, although one at Limiter 3 had a 16 cm diameter (to match the width of the limiter). These filtered line emission measurements (see Figure 4b) are used to determine neutral and impurity densities and particle fluxes. Good temporal resolution (100 kHz) yields detailed time-traces for each shot.

2.2 IR Calorimetry

The high resolution FLIR camera could resolve 10 milli-Kelvin temperature differences, so it was useful to make calorimetry measurements of bulk tile temperature changes, due to the integrated energy deposited, on a shot-by-shot basis. The IR camera measures a surface temperature during the shot, but by several minutes after a shot (in particular, immediately before the next pulse begins) it sees this turn into a bulk temperature. Individual tiles are well-insulated from each other, so we can record six different bulk temperature readings, one for each of tiles 2 through 6 on Limiter 3. By observing the decay rate of the bulk tile temperature (-6°C/1000 seconds at the end of the day) through the mounting brackets to the vessel wall,

we can correct the bulk tile temperature observed a few minutes after the shot, to what it would have been immediately at the end of the previous shot. Therefore, taking into account the tile heat capacities, we could directly measure the energy absorbed by each tile. While we could only see 5 of the 9 tiles on Limiter 3, we also had poloidal symmetry information from Limiter 5, where we could see the entire length of one side of the limiter. The up-down temperature symmetry was quite good [4]. Table 1 shows an example calculation of the energy absorbed by Limiter 3, during a 6-second shot (20160309.006) with ECRH input energy of 1 MW for 1 second and 0.6 MW for 5 seconds (total of 4 MJ energy).

Tile	Cp kJ/°K	ΔTc °C	E kJ	±ΔE
1	1.49	(28)	(42)	6
2	1.21	32.6	39.4	1
3	1.13	35.4	40.0	1
4	1.05	37.6	39.5	1
5	1.25	35.1	43.9	1
6	1.05	34.1	35.8	1
7	1.13	(35.4)	(40.0)	4
8	1.21	(32.6)	(39.4)	4
9	1.49	(28)	(42)	6
Sum			362	±25 kJ

Table 1. Energy absorbed by Limiter 3 during a 6-second, 4 MJ discharge (20160309.006). Quantities in parenthesis are estimated by symmetry, and information from the Limiter 5 (full length) IR view.

2.3 Asymmetries

The near-IR camera on Limiter 1 saw much higher temperatures (up to 1000 °C) on high energy (4 MJ discharges, but always after the plasma was over, to eliminate contamination from interfering plasma light) than IR views of Limiters 3 and 5. Furthermore, slow thermocouples in the back of the limiter mounting brackets provided additional toroidal symmetry information, indicating Limiter 1 was hotter by a factor of 1.9x than Limiter 3, and that Limiters 2, 4, and 5 were similar to each other. Overall, a multiplier of 7x times the power/energy incident on Limiter 3 (rather than 5x if fully symmetric), is our best estimate for the power/energy which flowed to the limiters. As a result, in the previous example (shot 20160309.006), we calculate that 2.5 MJ went to the limiters, or 62±10% of the microwave input energy. But using the same methodology, high-power (4 MW), 1-second shots had only ~35% of the energy going to the limiters. In discharges with heavy gas puffs (density ramps), the fraction to the limiters was as low as 20%. Notably, the bolometer system saw more radiation, and higher radiated power fractions in the high-power discharges, and a lower fraction in the low-power long-pulse discharges [8].

Post-run limiter inspection also revealed that the plasma interaction with Limiter 1 was qualitatively different, in the observed erosion/deposition pattern, compared to all of the other four limiters. In particular, the dark stripe pattern was covered over on the middle tiles of Limiter 1. This can be seen in Figure 5, where Limiter 1 and 5 are photographed side-by-side in the laboratory. This is another piece of evidence that Limiter 1 had a different (more intense) plasma interaction when compared to the other limiters.

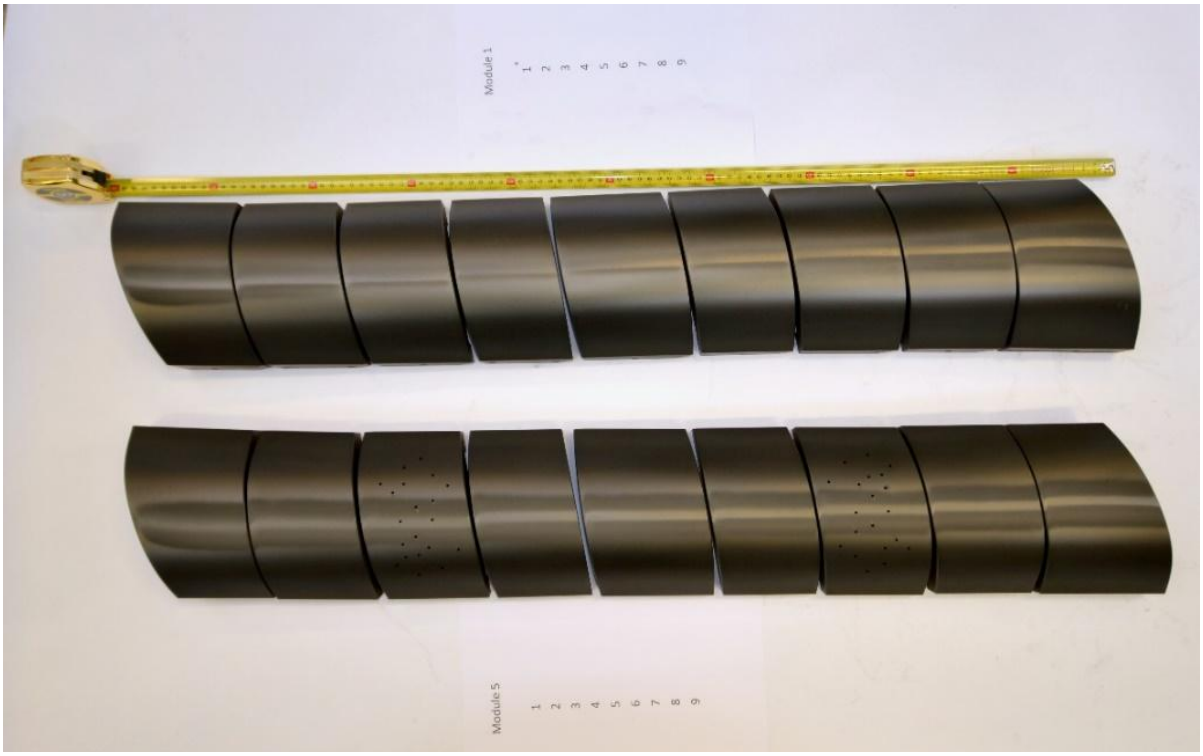

Figure 5. Overhead photo of Limiter 1 and Limiter 5 in the lab after the run, showing a large difference in the deposition/erosion pattern on the central tiles of Limiter 1, compared to Limiter 5.

Figure 6. Poloidal (top-bottom) asymmetry on all five limiters. Erosion/depostion patterns stop before the top tile, (with a small curvature to the right), but extend straight off the bottom tile, (with a small curvature to the left).

In addition to the observed toroidal asymmetry, post run visual examination of each limiter (Figure 6) revealed that at the bottom of the limiters, the erosion pattern extended straight off the lowest tile (#9), whereas at the top of the limiter (on tile #1), the pattern did not reach the end of the tile, and furthermore it curved off slightly to the right. The interaction could be "low" on the limiters, either due to the effect of particle drifts, or an actual vertical displacement, which would have to be a few centimetres.

3. Power fluxes

Time history of limiter power fluxes were calculated using IR surface temperature input data as a function of time, using the THEODOR [9] code, combined with temperature-dependent thermal properties of the high-density graphite tiles. An example of peak power flux on the left power stripe is shown in Figure 7 for a low power 0.6 MW shot. For 4 MW discharges, heat fluxes were ~5 MW/m^2 (as in Figure 2).

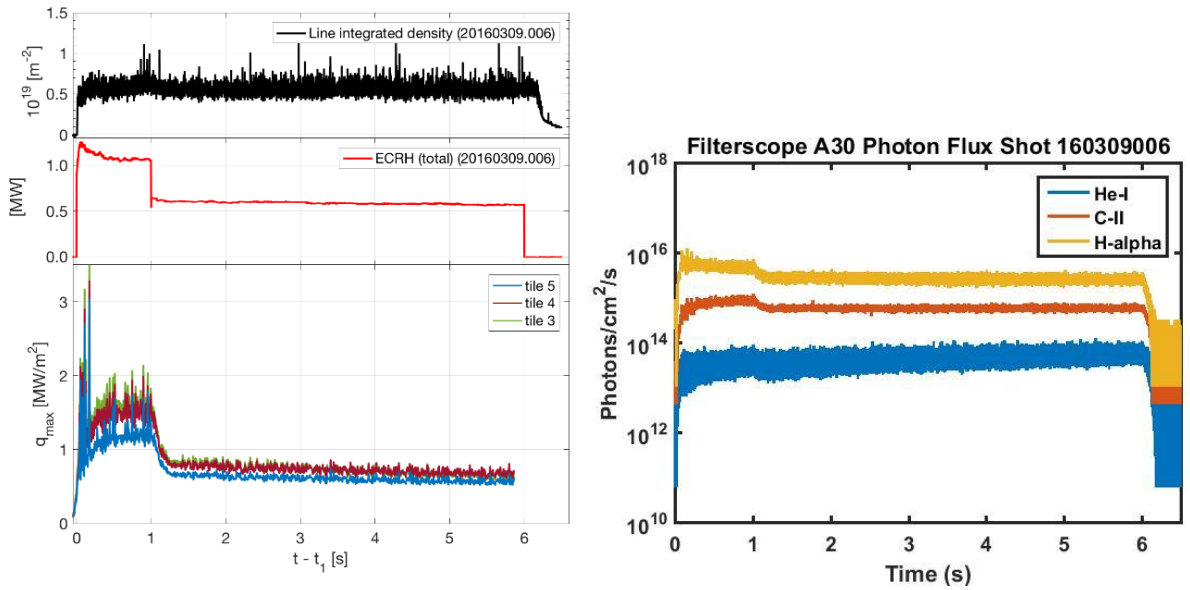

Figure 7. (left) Line averaged density, ECRH power are shown, along with power flux on the left-side heat stripe (Limiter 3) calculated with data for three tiles from IR thermography images over time using THEODOR, for a long duration discharge. (right) Corresponding nearly steady-state filterscope traces.

4. Modeling comparisons

Heat is carried to the limiters in the 3D scrape-off layer by primarily by particles carried by 3 different flux tube groups with different connection lengths: L_c = 36 m, 43 m, 79 m (the length depending whether you go once around the torus, or twice to the same or neighboring limiters) [2]. An example with IR measurements in Module 3 and direct comparisons to EMC3-EIRENE modelling [7] is shown in Figure 8. This provided evidence for the expected heat and particle flux asymmetries onto the limiters, indicating a 3-D helical scrape-off layer (SOL) was established [1]. The available modelling results also indicate a substantial broadening of the heat flux width with increasing perpendicular transport coefficient. Initial fits indicate a global diffusivity in the range of ~ 1 m^2/second. More refined estimates are in-progress, utilizing geodesic mapping of the curved limiter surface to scrape-off layer coordinates.

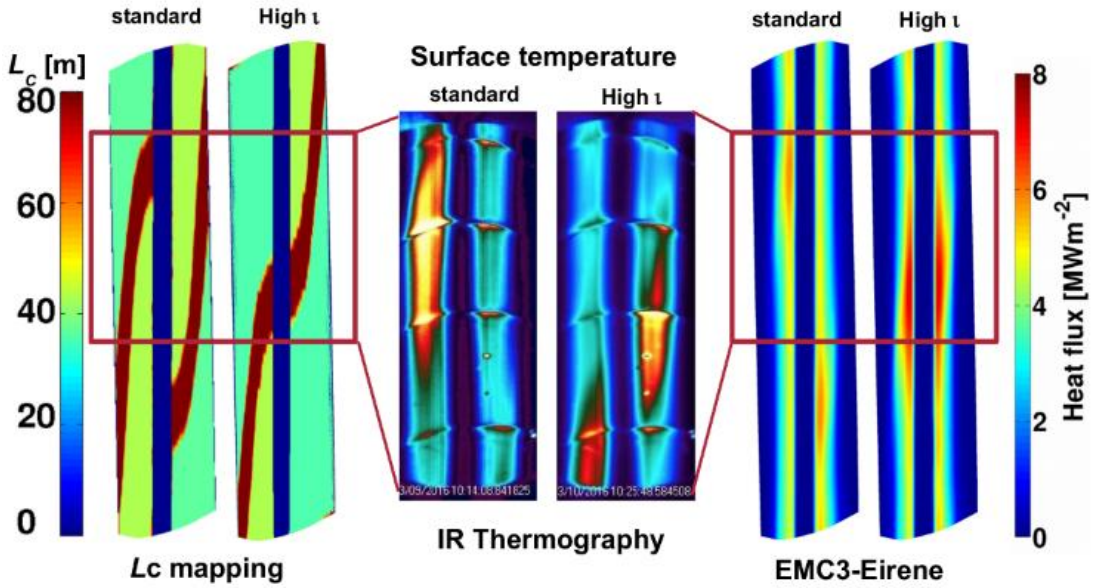

Figure 8: Different length flux tubes are mapped onto the limiter surface (left). Infrared heating patterns Temperature from IR images (middle) compared with EMC3-EIRENE modelling. Qualitatively, the asymmetry and region of higher heating matches with the model for both standard, and higher iota discharges.

The heating pattern on the limiters shifted in both the EMC3-EIRENE model prediction, and in the experiment, when we tried a new magnetic geometry in the last two days of OP1.1 operation. This is due to the change in magnetic topology, shown in the connection length mapping depicted on the left part of Figure 8. The basic behaviour of the heating moving from the left stripe, to the right stripe was as predicted (and also seen with other cameras). But in more detail, the code predicts a symmetric pattern on tile 5, while in the experiment (middle image), we see the left-right symmetry breakpoint about 3 cm below the centreline of tile 5.

5. Surface changes

Over the course of the three months of operation, evidence for surface modifications of the tiles became apparent during the latter half of the run. Inspection of the tiles after the end of OP1.1 operations was very informative. In particular, the infrared emissivity of the graphite tiles, which was nominally a uniform 0.82 before the campaign, became altered by erosion and deposition, depending on location on the surface. Here in Figure 9 is a visual close-up of three tiles (#3,4, &5) from Limiter 3, and a mid-IR image of tile 5 (right) when it was at a uniform temperature in the laboratory.

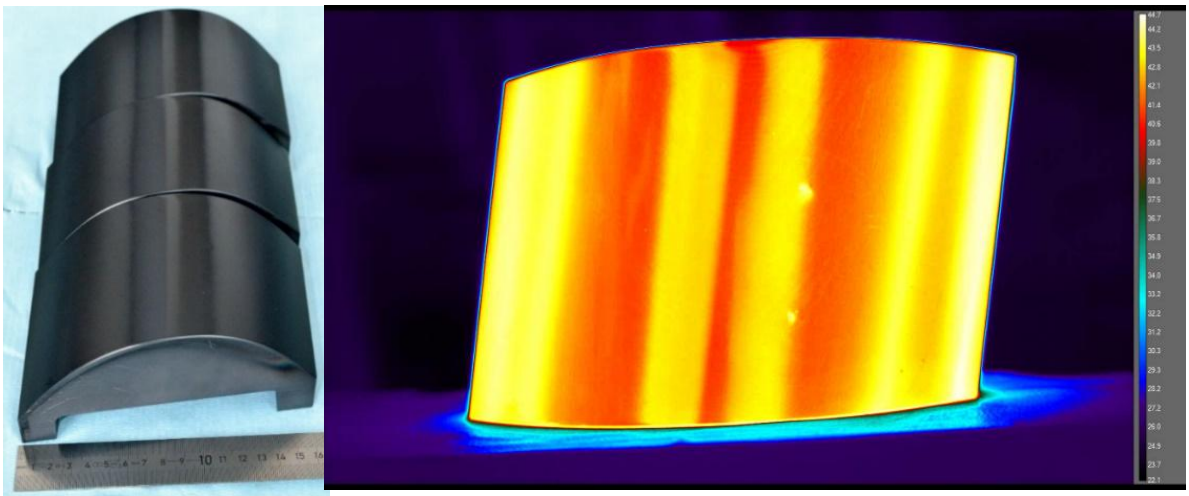

Figure 9. (left) Post OP1.1 visual close-up of tiles 3, 4 & 5 from Limiter 3. (right) The IR image of Limiter 3, middle tile (#5), in the laboratory at uniform temperature in air, showing variations in apparent temperature due to changes in emissivity. IR emissivity values correspond to red ~0.82, yellow ~0.95, and white is 1.00

The dark regions (visible image) did not align with the zone of maximum heating power, but were to the inner part of each heat stripe. The shiny regions (in the visible) in the heat stripes have an IR emissivity of ~0.82 (the same as the original tile material), but the rougher regions (darker in the visible, yellow in the IR) have a higher IR emissivity ~0.95. Far to the sides of the tiles there are regions of deposition, with IR emissivity values climbing to 1.00. Note also the two persistent defect spots on this tile. Detailed microscopic tile surface analysis is in progress in Jülich [10].

6. Transients

"Bursty" behavior of the limiter heating was apparent in some discharges. Although the FLIR camera basic full frame rate is 125 Hz, we routinely ran it with a sub-frame rate of 424 Hz, with exposure times ranging from 0.5 milliseconds down to 40 microseconds. This enabled us to see faster events, although we couldn't necessarily follow them from frame to frame. We did see indications of filamentary transient heating bursts close to the watershed, at > 1 kHz frequency, as shown in Figure 10.

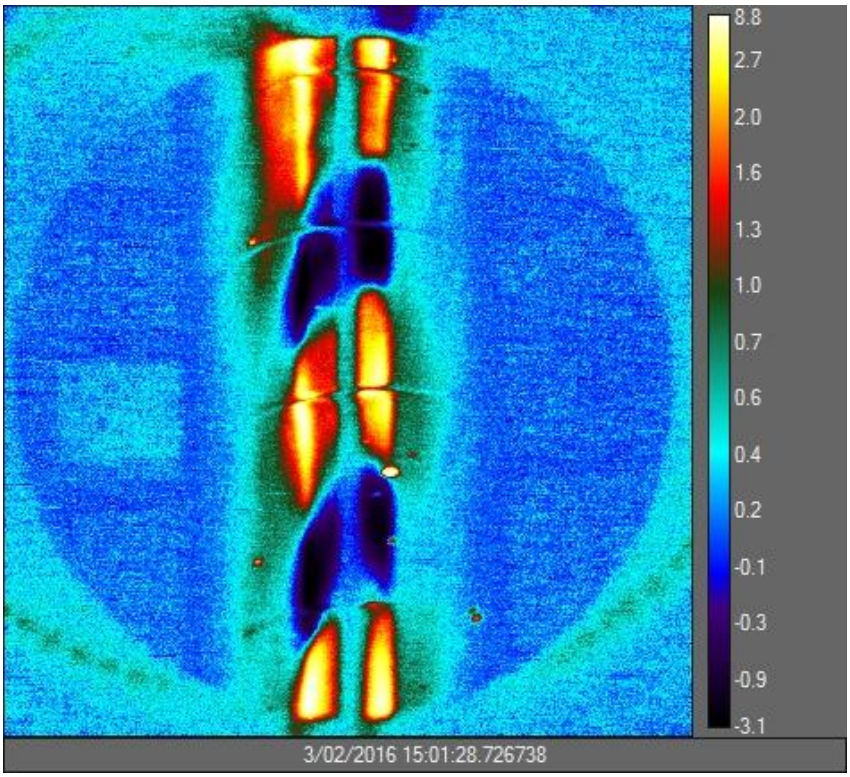

Figure 10. Using a sliding frame subtraction technique, we enhance the visibility of high frequency differential temperature (energy) bursts.

We noticed this effect most noticeably early in time in higher performance discharges. The visibility of bursts was also enhanced over the course of the last 3-4 weeks of OP1.1, by the development of surface coatings near the power stripes. These (weakly coupled) surface layers had the effect of enhancing the visibility of fast transient heat pulses because they could heat up and cool down more quickly than the bulk material. The m-number of these structures is high (m ~15), and they are frame-to-frame heat pulses with $\Delta T \sim 1$ - 60 °C. We are still investigating what is responsible for these events.

Another form of transients involved the detection of flying dust (UFO's) by the FLIR IR camera (across multiple frames), in about 5 % of the discharges, often in the first few shots of the morning (following helium discharge cleaning). Some were seen to originate on the graphite limiter, but others started outside of the AEA30 port field of view, evidently from metallic regions of the vessel.

7. Summary

We have been able to characterize heat fluxes on the poloidal limiters in W7-X during the first helium and hydrogen plasmas during OP1.1. Dual heating stripes, with patterns to a large degree matching modelling predictions, were observed. IR thermography and calorimetry using multiple IR camera systems, combined with slow thermocouples to account for toroidal asymmetries, allowed us to estimate that the limiters intercepted up to 60% of the total energy put into the vessel by the ECRH heating system for low power (0.6 MW) long pulse (6 second) shots, and a smaller fraction (~35%) for high power (4MW) short duration (1 second) discharges. The use of trim coils to affect the limiter heat loads is described in other papers (S. Lazerson, et. al., EX/P5-5 and S. Bozhenkov EX/P5-8) at the IAEA FEC 2016, Kyoto, Japan.

Acknowledgements

Acknowledgement & Disclaimer: This work has been funded under DOE LANS Contract DE-AC52–06NA25396 and Office of Science grant DE-SC0014210. This work has also been carried out within the framework of the EUROfusion Consortium and has received funding from the Euratom research and training programme 2014-2018 under grant agreement No 633053. The views and opinions expressed herein do not necessarily reflect those of the European Commission.

References

[1] T. Sunn Pedersen et al., “Plans for the first plasma operation of Wendelstein 7-X”, Nuclear Fusion, 55, 126001 (2015).

[2] S. A. Bozhenkov, F. Effenberg, et al, “Limiter for the early operation phase of W7-X”, 41st EPS Conf. on Plasma Physics, P1.080, Berlin (2014). http://ocs.ciemat.es/EPS2014PAP/pdf/P1.080.pdf

[3] M. Krychowiak, et. al., “Overview of diagnostic performance and results for the first operation phase in Wendelstein 7-X”, Rev. Sci. Instrum. 87, 11D304 (2016); http://dx.doi.org/10.1063/1.4964376 .

[4] G. A. Wurden, L. A. Stephey, et. al., "A high resolution IR/visible imaging system for the W7-X Limiter", Rev. Sci. Instrum. 87, 11D607 (2016); http://dx.doi.org/10.1063/1.4960596

[5] H. Niemann, M. Jakubowski, et. al., “Power loads in the limiter phase of Wendelstein 7-X”, 43rd EPS Conf. on Plasma Physics, P4.005, Belgium (2016). http://ocs.ciemat.es/EPS2016PAP/pdf/P4.005.pdf

[6] L. A. Stephey, G. A. Wurden, et al., “Spectroscopic imaging of limiter heat and particle fluxes and the resulting impurity sources during Wendelstein 7-X startup plasmas”, Rev. Sci. Instrum. 87, 11D606 (2016). http://dx.doi.org/10.1063/1.4959274

[7] F. Effenberg et al., “Numerical investigation of edge transport and limiter heat loads in Wendelstein 7-X startup plasmas”, submitted for publication in Nuclear Fusion 2016.

[8] D. Zhang, R. Burhenn, et. al., “Investigation of the Radiative Power Loss in the Limiter Plasmas of W7-X”, 43rd EPS Conf. on Plasma Physics, P4.015, Belgium (2016). http://ocs.ciemat.es/EPS2016PAP/pdf/P4.015.pdf

[9] Herrmann, A. et al., Plasma Phys. Control. Fusion 37, 17 (1995).

[10] Winters, V. et al., BAPS, APS-DPP meeting, San Jose, CA, Nov. 3-8, 2016.